

SELECTIVE ADSORPTION OF U(VI) BY USING U(VI)-IMPRINTED POLY-HYDROXYETHYL METHACRYLATE-METHACRYLOYL-L-HISTIDINE (P-[HEMA-(MAH)₃]) CRYOGEL POLYMER

DOLAK, İ.

*Vocational School of Technical Sciences, Dicle University, Diyarbakır, Turkey
(e-mail: idolak@dicle.edu.tr; phone: +90-542-531-2121)*

(Received 3rd Jan 2019; accepted 8th Feb 2019)

Abstract. In this study, selective adsorption of U(VI) in aqueous solutions in the presence of various lanthanide ions was conducted by using U(VI)-imprinted cryogel polymer. For this purpose, the pHEMA-(MAH)₃-U(VI) cryogel polymer was prepared by free radical polymerization method. U(VI) was desorbed with 5.0 mol.L⁻¹ HNO₃ and thus U(VI)-imprints were created on p-HEMA-(MAH)₃ cryogel polymer. To determine the optimum conditions, in the process of selective adsorption of U(VI) ion to U(VI)-imprinted p-HEMA-(MAH)₃ cryogel polymer, some parameters such as pH, flow rate, initial U(VI) concentration were investigated. Under the optimum conditions, the maximum adsorption capacity was obtained as 74.80 mg.g⁻¹. Selectivity studies were also carried out in the presence of Nd(III), La(III) and Y(III) ions using U(VI)-imprinted p-HEMA-(MAH)₃ cryogel polymer. The obtained adsorption order under competitive conditions was U(VI) > La(III) > Y(III) > Nd(III).

Keywords: uranium, adsorption, ion imprinting, lanthanides, nuclear energy

Abbreviations: HEMA: 2-Hydroxyethyl methacrylate; MAH: N-methacryloyl-(L)-histidine methyl ester; TEMED: N,N,N,N-tetramethylethylenediamine; APS: Ammonium persulfate; MBAAm: N,N-methylenebisacrylamide; ICP-MS: Inductively Coupled Plasma-Mass Spectroscopy; SEM: Scanning Electron Microscopy; FT-IR: Fourier Transform Infrared; IIP: Ion Imprinting Polymer; NIP: Non Imprinting Polymer

Introduction

Uranium is an important material in nuclear science and an important actinide in radioactive waste water and environmental samples (Wang et al., 2017a). Uranium is a natural element that quite effective in the nuclear industry and particularly as a fuel for electricity generation by nuclear power plants (Iliaa et al., 2017). Studies on uranium-containing rare earth minerals are causing uranium-containing radioactive pollutants (Li et al., 2018; Wang et al., 2017b; Lu et al., 2016; Wang et al., 2015). Therefore, the solvent extraction and separation of Uranium from rare earth minerals is quite important for the environmental protection (Zhu et al., 2015).

Uranium is the most important fuel element used in nuclear reactors. Therefore, the recovery of Uranium is of great importance for the sustainable development of nuclear industry (Gu, 2007). The content of uranium in the earth's crust is limited (Abdollahy et al., 2011). Anticipating the shortage of nuclear fuels in near future, the selective recovery of Uranium becomes necessary for the sustainable development of nuclear energy (Chmielewski, 2008).

The removal of uranium from the body has been studied by a number of investigators. Mostly, the low concentrations of uranium encountered and the presence of high levels of interfering matrix constituents prevent its direct determination. Because of this, various separation and preconcentration techniques are employed for the determination of uranium. Although liquid-liquid extraction has been widely used

(Horwitz et al., 1992), it is time consuming. Extraction chromatography (Dolak, et al., 2011), solid-phase extraction (Yener et al., 2017; Kaminski et al., 2000), supercritical fluid extraction (Haerizade et al., 2018), ion exchange (Dolak et al., 2010) and adsorbents (İnam et al., 2001; Sana et al., 2015) have been extensively used for the separation and preconcentration of uranium ions. The process of using adsorbents is an effective method for heavy metals by using metal chelating resins prepared with containing aminoacid monomer ligands (Dolak et al., 2015; Keçili et al., 2018; Dolak, 2018), and for recovering uranium because of the high selectivity for uranium, the ease of handling, and environmental safety. The solid-phase extraction methods using molecular imprinted polymers are the most used methods for the separation and preconcentration of rare earth elements (Harkins and Schweitzer, 1991; Panahi et al., 2012; Wulff, 1995).

Molecular imprinting is a method for making selective binding sites in synthetic polymers by using molecular template. Metal cations can be used as templates for imprinting crosslinked polymers. After the removal of template (the cation), the remaining polymer is more selective. The selectivity of the polymer depends on various factors, like the charge on the cation, the size of the cation, the specificity of the interaction of the ligand, the coordination geometry, and the number of the cations. Transition metals can also be removed by using the molecular imprinting method (Pakdehi, 2016; Dhal and Arnold, 1992; Chen et al., 2017).

Molecular imprinting is a new technique has attracted the attention of researchers for effective recognition of chemical and biological molecules including aminoacids, proteins, enzymes, DNA, drugs and metal ions (Didaskalou et al., 2017; Székely et al., 2012a, b; Dolak et al., 2018). This technique allows selective and sensitive recognition of chosen target molecule by leaving artificial imprinted cavities in polymer matrix that provides high affinity to target molecule. To synthesize molecularly imprinted polymer, the template molecule and functional monomers which can arrange around template are complexed interactively before polymerization. Then the rigid polymer matrix is obtained by polymerization of formed pre-complex and cross-linker reagent. After removal of template molecule from the polymer with suitable desorption agent, the cavities remaining in the polymer that are complementary in shape, size and chemical functionality to the template. Consequently, the resultant polymer able to recognizes and rebinds selectively the template or other molecules that are chemically related to the template (Saylan et al., 2017). This technique is used in many applications such as selectivity recognition and separation (Sellersgren, 2001; Wei and Mizaiakoff, 2007; Vedadghavami et al., 2018; Lasáková and Jandera, 2009), drug delivery systems (Alvarez-Lorenzo and Concheiro, 2004), catalysis (Vidyasankar and Arnold, 1995), sensor technology (Monier and Abdel-Latif, 2017). In addition, ion imprinted polymers (IIPs) have been used for the selective removal of metal ions from different matrices (Moussa et al., 2016; Moorthy et al., 2013; Monier et al., 2016; Mitreva et al., 2017; Msaadi et al., 2017; Roushani et al., 2015; Fayazi et al., 2016; Candan et al., 2009; Gao et al., 2015).

In this study, the selective adsorption of U(VI) in aqueous solutions and soil certified reference material in the presence of other lanthanide ions such as Nd(III), La(III) and Y(III) was performed by using U(VI)-imprinted pHEMA-(MAH)₃ cryogel polymer purposed. For this purpose, U(VI) was complexed with N-methacryloyl-L-histidine methyl ester (MAH) and the prepared (MAH)₃-U(VI) complex monomer was polymerized with 2- hydroxyethyl methacrylate (HEMA) cryogel to prepare pHEMA-

(MAH)₃-U(VI) cryogel polymer by free radical polymerization method. U(VI) was desorbed with 5.0 mol.L⁻¹ HNO₃ and thus were created U(VI) imprinted on to p-HEMA-(MAH)₃ cryogel polymer. In the process of selective adsorption of U(VI) ion to U(VI)-imprinted p-HEMA-(MAH)₃ cryogel polymer, several factors such as medium pH, flow rate, initial U(VI) concentration were investigated to determine optimum conditions. Selectivity studies were also carried out in the presence of Nd(III), La(III) and Y(III) ions using U(VI)-imprinted p-HEMA-(MAH)₃ cryogel polymer. The obtained adsorption order under competitive conditions was U(VI) > La(III) > Y(III) > Nd(III).

Materials and methods

Chemicals and reagents

The chemicals used in the study and their properties are given in *Table 1*.

Table 1. Used chemicals and their properties

Chemicals	For what	Manufacturer
Methacryloyl chloride	For monomer synthesis	Sigma Aldrich-Steinheim, Germany (purum, dist., ≥97.0% (GC), contains ~0.02% 2,6-di-tert-butyl-4-methylphenol as stabilizer)
L-histidine	For monomer synthesis	Sigma Aldrich-Steinheim, Germany (ReagentPlus®, ≥99%)
2-Hydroxyethyl methacrylate (HEMA)	For polymer synthesis	Sigma Aldrich-Steinheim, Germany (≥99%, contains ≤50 ppm monomethyl ether hydroquinone as inhibitor)
N,N,N,N-tetramethyl ethylene diamine (TEMED)	For polymer synthesis	Sigma Aldrich-Steinheim, Germany (BioReagent, suitable for electrophoresis, ~99%)
N,N-methylenebisacrylamide (MBAAm)	For polymer synthesis	Sigma Aldrich-Steinheim, Germany (99%)
Ammonium persulfate (APS)	For polymer synthesis	Sigma Aldrich-Steinheim, Germany (reagent grade, 98%)
Uranyl nitrate	For experimental optimization studies	Sigma Aldrich-Steinheim, Germany (extra pure, ≥99%)
Lanthanum(III) nitrate hexahydrate	For selectivity study	Sigma Aldrich-Steinheim, Germany (extra pure, ≥99%)
Neodymium(III) nitrate hexahydrate	For selectivity study	Sigma Aldrich-Steinheim, Germany (extra pure, ≥99%)
Yttrium(III) nitrate hexahydrate	For selectivity study	Sigma Aldrich-Steinheim, Germany (extra pure, ≥99%)
All organic solvents	For synthesis imprinted polymer	Sigma Aldrich-Steinheim, Germany

Instrumentation

The analysis of the U(VI) and the other lanthanide ions was performed using a Agilent 7700 Series inductively coupled plasma-mass spectroscopy (ICP-MS). System

with the following parameters: RF Power = 1600 W, sampling depth = 5.3 mm, analyzer pressure = 7.92×10^{-5} Pa, helium flow in the collision cell = 4.98 mL.min⁻¹ and plasma temperature = 9883 K. The measurements were done with three replicates (95% confidence level). A Perkin Elmer model Spectrum 400 FT-IR spectrometer was used for the Fourier transform infrared (FT-IR) measurements. Scanning electron microscopy (SEM) analyses were carried out by using a FEI Quanta FEG 250 SEM system.

Preparation of U(VI)-imprinted and non-imprinted p-HEMA-(MAH)₃ cryogel polymer

Synthesis of N-methacryloyl-L-histidine methyl ester (MAH)

The preparation and characterization of N-methacryloyl-(L)-histidine methyl ester (MAH) was reported elsewhere (Berefi et al., 2011). The following procedure was applied for the synthesis of MAH monomer: 5.2 g of L-histidine methylester and 0.22 g of hydroquinone were dissolved in 150 mL of CH₂Cl₂ solution. Solution was cooled down to 0 °C. 12.83 g triethylamine was added to the solution. 4.0 mL of methacryloyl chloride was poured slowly into this solution under nitrogen atmosphere and then this solution was stirred magnetically at room temperature for 1 h. At the end of this chemical reaction period, unreacted methacryloyl chloride was extracted with 10% NaOH. Aqueous phase was evaporated in a rotary evaporator. MAH was crystallized in 20 mL (1:1) ethanol and ethyl acetate. The reaction efficiency was determined as 84% in the stoichiometric calculations based on the amount of reagents added to the reaction medium and the amount of MAH monomer obtained as a result of the process. In addition, it was determined that the purity of MAH monomer synthesized as a result of the characterization processes was greater than 98%.

Preparation of (MAH)₃-U(VI) complex monomer

For preparation (MAH)₃-U(VI) complex monomer, MAH (0.669 mg, 3.0 mmol) was dissolved in deionized water. After slow addition of UO₂(NO₃)₂ (0.394 mg, 1.0 mmol) to this solution, the solution was stirred for 24 h at room temperature. The obtained complex monomer was then filtered and extensively washed with EtOH and deionized H₂O. Then, it was dried at 50 °C for 24 h. For the yield of the synthesis of the synthesized MAH-Th(VI) complex monomer, it was initially determined by ICP-MS analysis of the remaining Th(VI) in the medium which was added to the medium and the complex formation yield was determined to be greater than 95%.

Synthesis of p-HEMA-(MAH)₃-U(VI) (IIP) and p-HEMA-(MAH)₃ (NIP) cryogel polymer

p-HEMA-(MAH)₃-U(VI) and p-HEMA-(MAH)₃ cryogel polymers were prepared according to a previously reported method (Baysal et al., 2018). For this purpose, 0.25 g MBAAm was dissolved in deionized H₂O, and then 2.0 mL HEMA and 2.0 mL (MAH)₃-U(VI) complex monomer were mixed with this solution. Initiator APS (25 mg)/TEMED (25 µl) was added and the final mixture was placed into a syringe closed with parafilm and allowed to polymerize at -18 °C for 24 h. The frozen solution was allowed to thaw at room temperature. Finally, the prepared imprinted cryogel polymer was washed with 100 mL (1:1) EtOH and deionized H₂O to remove impurities, which was then stored at +4 °C. Non-imprinted polymer were prepared in the same way but in the absence of the template.

Removal of U(VI) from p-HEMA-(MAH)₃-U(VI) cryogel polymer

To obtain the 3-D cavities for desorption of U(VI), the template U(VI) was successfully desorbed from the p-HEMA-(MAH)₃-U(VI) cryogel polymer (Fig. 1). For this purpose, the cryogel polymer was desorbed with 10 mL 5.0 mol.L⁻¹ HNO₃ as the desorption solvent for 1 h by using a peristaltic pump. This washing step was repeated until no U(VI) was determined in the desorption solvent.

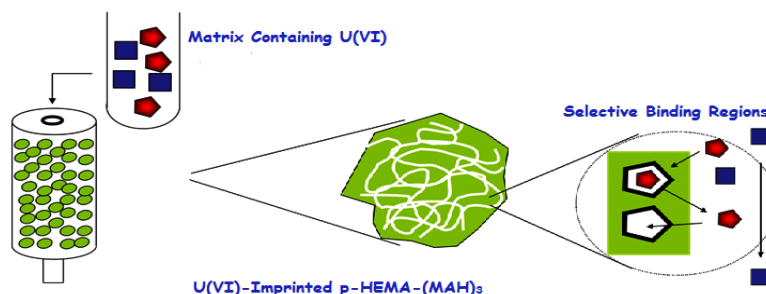


Figure 1. The prepared U(VI)-imprinted column system and selective separation scheme of U(VI)

Figure 1 shows schematically that only U(VI) is selectively bound when the mixture of La(III), Nd(III), Y(III) and U(VI) is passed through a prepared U(VI) imprinted p-HEMA-(MAH)₃ cryogel column.

Characterization studies

MAH monomer and prepared (MAH)₃-U(VI) complex monomer were characterized by FT-IR spectroscopy, whereas U(VI)-imprinted p-HEMA-(MAH)₃ cryogel polymer were characterized by FT-IR spectroscopy and SEM technique.

To obtain FT-IR spectrum U(VI)-imprinted p-HEMA-(MAH)₃ cryogel polymer, KBr was mixed with the dried polymer particles and pressed into a pellet form, and the spectra were then recorded.

For the SEM analysis of U(VI)-imprinted p-HEMA-(MAH)₃ cryogel polymer were covered on the surface of platinum and coated with gold (thickness of 20 nm). Then, SEM analyses were carried out.

To calculate the swelling ratio of p-HEMA-(MAH)₃ cryogel polymer, the cryogel was dried and weighed until constant weight (m_{dried}). Then, it was placed in a 30 mL vial containing distilled water and kept at 25 °C for 2 h. The cryogel was removed from water, wiped by a filter paper and weighed again (m_{wet}). The swelling ratio was calculated according to Equation 1:

$$S = m_{\text{wet}} - m_{\text{dried}} / m_{\text{dried}} \quad (\text{Eq.1})$$

For the measurement of macroporosity percentage (M%) of cryogels, the mass of water-saturated cryogels (m_{wet}) was weighed. The cryogel was squeezed to remove free water which is found in the pores (m_{squeezed}), and the mass of cryogel without water was weighted. M% was calculated according to Equation 2:

$$M\% = m_{\text{wet}} - m_{\text{squeezed}} / m_{\text{wet}} \quad (\text{Eq.2})$$

Adsorption studies of U(VI) ion to U(VI)-imprinted (IIP) and non-imprinted (NIP) cryogel polymer

Continuous column system was used to adsorption U(VI) to U(VI)-imprinted p-HEMA-(MAH)₃ cryogel polymer (IIP) and non-imprinted p-HEMA-(MAH)₃ cryogel polymer (NIP). For this purpose, firstly, columns containing IIP and NIP was washed with deionized H₂O and equilibrated with 0.1 mol.L⁻¹ phosphate buffer at pH. 7.0. Then, aqueous solution of U(VI) was passed through the columns containing IIP and NIP at 1 mL.min⁻¹ flow rate for 1 h. The amounts of U(VI) was determined by ICP-MS. Then, 5.0 mol.L⁻¹ HNO₃ was used to desorption of U(VI) bound to the IIP and NIP. Several factors such as pH, flow rate and initial U(VI) concentration were also investigated to obtain the optimum conditions for the adsorption of U(VI). 10 ppm U(VI) solutions in different pH values (pH 3 to 10) was passed through the columns containing IIP and NIP at 1 mL.min⁻¹ flow rate for 1 h in order to test pH influence on U(VI) adsorption to the IIP and NIP. Then, the samples came out from the column were analyzed by ICP-MS. The flow rates between 1.0 mL.min⁻¹ and 5.0 mL.min⁻¹ were applied for the investigation of the effects of these parameters on the adsorption of U(VI). The initial U(VI) concentration was varied between 10 ppm and 2000 ppm to determine maximum adsorption capacity.

Selectivity study

The selectivity of the prepared U(VI)-imprinted (IIP) and Non-imprinted NIP cryogel polymers toward U(VI) were investigated in the presence of U(VI)-Nd(III), U(VI)-La(III) and U(VI)-Y(III) ion pairs. For this purpose 25 mL of 10 ppm lanthanide solutions in 10 mM phosphate buffer, pH 7.0 were passed from columns containing IIP and NIP at a flow rate of 1 mL.min⁻¹ at room temperature. Analysis of the lanthanide ions in the column output samples was performed by ICP-MS.

The distribution coefficient of U(VI) ion between the columns containing IIP and NIP and aqueous solutions was calculated using *Equation 3*:

$$K_d = (C_i - C_f / C_f) \times (V/m) \quad (\text{Eq.3})$$

where K_d is the distribution coefficient, C_i is initial U(VI) concentration and C_f is final U(VI) concentration, V represents the solution volume (mL) and m is the polymer mass (g).

The selectivity coefficient (k) and relative selectivity coefficient (k^1) for U(VI) in the presence of other competing lanthanide ions can be calculated applying *Equations 4* and *5*:

$$k = K_{(U(VI))} / K_{(\text{interfering ion})} \quad (\text{Eq.4})$$

$$k^1 = K_{(\text{imprinted})} / K_{(\text{nonimprinted})} \quad (\text{Eq.5})$$

where $K_{(U(VI))}$ is the distribution ratio of U(VI) ion and $K_{(\text{interfering ion})}$ is the distribution ratio of potentially interfering ions.

Reusability of U(VI)-imprinted cryogel polymer (IIP)

For the reusability studies, adsorption and desorption studies were repeated 10 times using same IIP. After each step, column was washed with 10 mL 5 mol.L⁻¹ HNO₃ and deionized water.

Adsorption studies of U(VI) ion from soil certified reference material

Soil certified reference material was selected as the real sample for the selective adsorption of U(VI). For this purpose, 0.1 g soil certified reference material powdered was leached using concentrated HNO₃ and H₂SO₄ by microwave irradiation. Then, solution pH was adjusted to 7.0 using phosphate buffer and volume of the final solution was distilled to 100 mL by deionized water. The prepared solution was passed through the columns containing IIP and NIP the under the optimum conditions. Analysis of the ions in the column output samples was performed by ICP-MS.

Results and discussion

Characterization of MAH monomer and (MAH)₃U(VI) complex monomer

Prepared (MAH)₃-U(VI) complex monomer were characterized by FT-IR spectroscopy, which proved that monomer and complex monomer were synthesized. The obtained FT-IR spectrum of the MAH monomer and (MAH)₃U(VI) complex monomer is given in Figure 2.

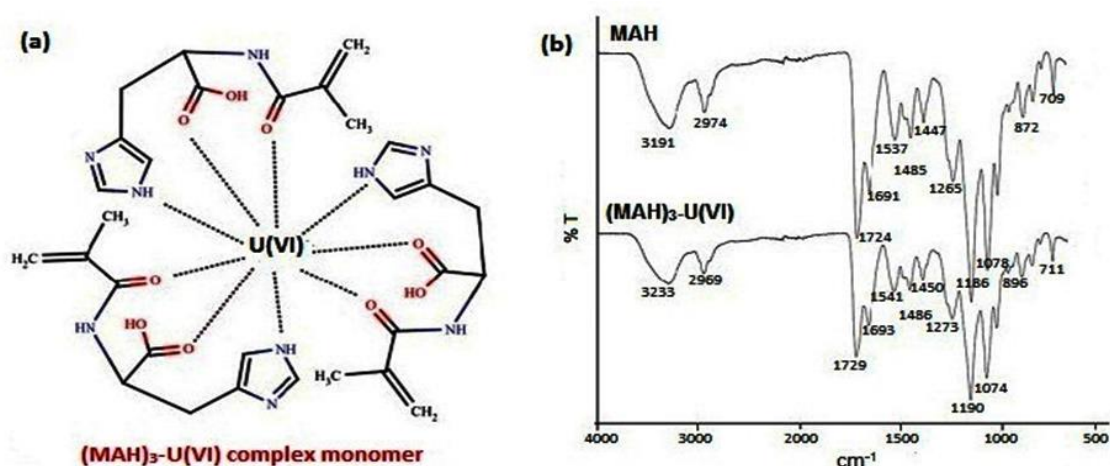


Figure 2. a Proposed structure for complex formed; b FTIR spectrum for the MAH monomer and (MAH)₃U(VI) complex monomer

Characterization of U(VI)-imprinted p-HEMA-(MAH)₃ cryogel polymer (IIP)

p-HEMA and Th(IV)-imprinted p-HEMA-(MAH)₃ cryogel polymer (IIP) were characterized by FT-IR and SEM. Figure 3 shows the FT-IR Spectra p-HEMA and U(VI)-imprinted p-HEMA-(MAH)₃ cryogel polymer. As can be seen, p-HEMA and U(VI)-imprinted p-HEMA-(MAH)₃ cryogel polymer exhibited FT-IR patterns with small differences which confirms the similar polymer backbone.

The pore structure and pore size of U(VI)-imprinted p-HEMA-(MAH)₃ cryogel polymer were visualized with SEM images as seen in Figure 4. As shown in Figure 3, the U(VI)-imprinted p-HEMA-(MAH)₃ cryogel polymer has interconnected pores and porous structure. Pore size was found about 50 μm.

The equilibrium swelling degree and macroporosity of the U(VI)-imprinted p-HEMA-(MAH)₃ cryogel were 6.12 g H₂O/g cryogel and 81.04%, respectively.

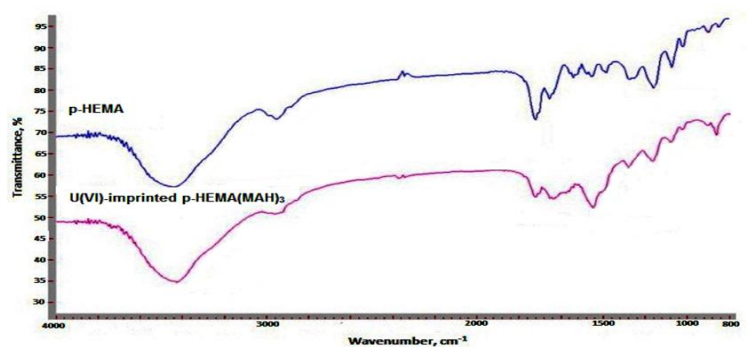


Figure 3. FT-IR spectrum p-HEMA cryogel and U(VI)-imprinted p-HEMA-(MAH)₃ cryogel polymer

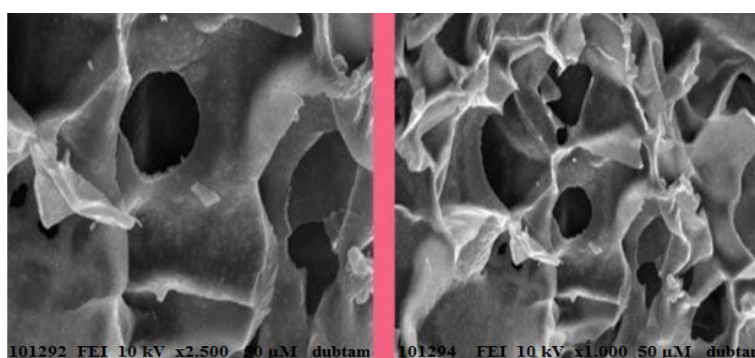


Figure 4. SEM images U(VI)-imprinted p-HEMA-(MAH)₂ cryogel polymer (IIP)

Adsorption studies of U(VI) on IIP and NIP

pH effect on U(VI) adsorption

The change in amount of U(VI) adsorption to the IIP and NIP as a function of pH was investigated, as seen in *Figure 5*. The maximum U(VI) binding to the IIP and NIP pH 7.0. This could be explained by electron transfer based covalent cross-linking between U(VI) and L-histidine of the functional monomer at pH 7.0. *Figure 5* clearly shows effect of pH on U(VI) binding to the IIP and NIP. As seen in the figure, the values higher and lower than pH 7.0 lead to low adsorption of U(VI) to the IIP and NIP, which can be explained by the repulsive electrostatic interactions between bound U(VI) ion and MAH monomer. The adsorption efficiency may decrease because of the size of conformation and the lateral electrostatic interactions between adjacent U(VI) ion on the IIP and NIP. The experiments were repeated 3 times and the statistical values were given as 95% confidence level relative standard deviation (RSD).

Flow rate effect on U(VI) adsorption

The flow rate of the U(VI) solution pumped through the cryogel is one of the crucial parameter for the control of binding process (Fayazi et al., 2016). The flow rate effect on the adsorption of U(VI) was explored by changing the flow rate from 1.0 to 5.0 mL.min⁻¹. 10 ppm U(VI) solution was used for this purpose. Owing to the back pressure produced by the column, the flow rates higher than 5.0 mL.min⁻¹ could not be

investigated. The experiments were repeated 3 times and the statistical values were given as 95% confidence level relative standard deviation (RSD). As shown in *Figure 6*, increasing flow rate resulted in a decrease in the adsorption of U(VI) from $96.56 \pm 1.52\%$ to $70.84 \pm 1.26\%$ adsorption capacity.

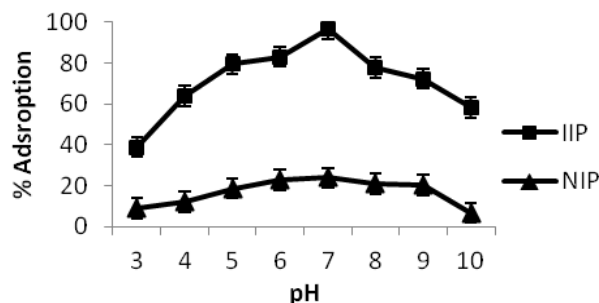


Figure 5. Effect of pH on U(VI) adsorption (experimental conditions: initial U(VI) concentration: 10 ppm; temperature: 25 °C; flow rate: 1 mL.min⁻¹; time: 1 h)

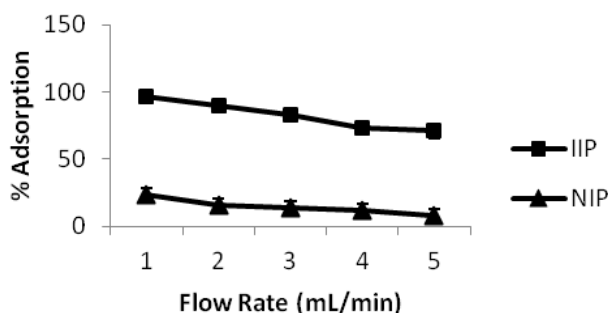


Figure 6. Effect of flow rate on U(VI) adsorption (experimental conditions: pH:5; initial U(VI) concentration: 10 ppm; temperature: 25 °C; time: 1 h)

The determination maximum adsorption capacity of IIP and NIP

Initial U(VI) concentration dependence of the bound amount of the U(VI) on to IIP and NIP is depicted in *Figure 7*. As can be seen *Figure 7*, U(VI) adsorption increased when initial U(VI) concentration is increased, and an equilibrium was obtained at a U(VI) concentration of 2000 ppm. The maximum adsorption capacity was obtained as 74.80 ± 1.33 mg.g⁻¹ for IIP, while that of NIP was 14.76 ± 1.09 mg.g⁻¹. The experiments were repeated 3 times and the statistical values were given as 95% confidence level relative standard deviation (RSD). It was found that maximum adsorption yield obtained was good result when compared to other studies (Iliaa et al., 2017; Li et al., 2018; Zhu et al., 2015).

Regeneration and reusability of the IIP

One of the crucial advantages for an affinity material for the recognition and separation processes is its reusability (Kupai et al., 2017). To test the reusability of the prepared IIP, U(VI) adsorption and desorption cycle was repeated 10 times using the same cryogel (*Fig. 8*). The elution of U(VI) from the IIP was performed by using 10 mL 5.0 mol.L⁻¹ HNO₃ as the desorption solution and complete removal of U(VI) was

achieved after the desorption step. It was found that the adsorption behavior of the IIP towards U(VI) did not change significantly after ten adsorption and desorption cycles. Thus, one can easily say that the IIP are stable and the IIP can be used many times without significant loss of their adsorption capacity.

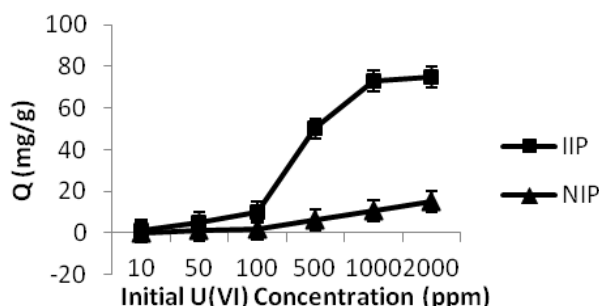


Figure 7. Effect of initial U(VI) concentration on Th(IV) adsorption (experimental conditions: pH:5; temperature: 25 °C; flow rate: 1 mL.min⁻¹; time: 1 h)

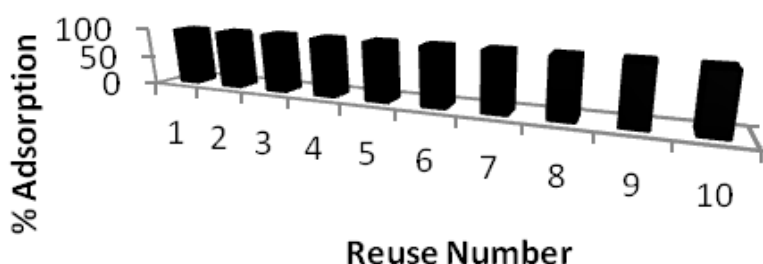


Figure 8. Reusability of IIP (experimental conditions: pH:5; initial U(VI) concentration: 10 ppm; temperature: 25 °C; flow rate: 1 mL.min⁻¹; time: 1 h)

Selectivity studies

Competitive adsorption of U(VI)-Nd(III), U(VI)-La(III) and U(VI)-Y(III) were also explored in a column system. The obtained results are given in Table 2. U(VI) imprinted cryogel polymer (IIP) exhibited higher selectivity toward U(VI) ions over Nd(III), La(III) and Y(III) ions. K_d values for the IIP were compared with NIP. The obtained results confirmed that the relative selectivity coefficients of the IIP for the U(VI)/Nd(III), U(VI)/La(III) and U(VI)/Y(III) were 129, 60 and 79 times higher than the corresponding NIP, respectively. As a result, it was found that the prepared U(VI)-imprinted cryogel polymer (IIP) exhibited a selectivity to U(VI) ion in the presence of other lanthanides.

Selective adsorption of U(VI) from soil certified reference material

The outcomes of the adsorption of U(VI) from certified reference material are given in Figure 9. The results showed that the IIP displayed $93.11 \pm 1.47\%$ adsorption toward U(VI) while NIP showed $18.74 \pm 0.91\%$ adsorption. The experiments were repeated 3 times and the statistical values were given as 95% confidence level relative standard deviation (RSD).

Table 2. K_d , k and k' values of Nd(III), La(III) and Y(III) with respect to U(VI) (experimental conditions: pH:5; temperature: 25 °C; flow rate: 1 mL.min⁻¹; time: 1 h)

Cryogel column U(VI) (ppm) Nd(III) (ppm) K_d (U(IV)) K_d (Nd(III)) k k'						
Non-imprinted	10	10	761.2	1972.1	0.38	-
U(IV)-imprinted	10	10	98090	2760.1	35.5	129
Cryogel column U(VI) (ppm) La(III) (ppm) K_d (U(IV)) K_d (La(III)) k k'						
Non-imprinted	10	10	1827.9	2633.5	0.70	-
U(IV)-imprinted	10	10	108155	2086.0	51.3	60
Cryogel column U(VI) (ppm) Y(III) (ppm) K_d (U(IV)) K_d (Y(III)) k k'						
Non-imprinted	10	10	927.8	2331.5	0.40	-
U(IV)-imprinted	10	10	73258	2041.0	36.0	79

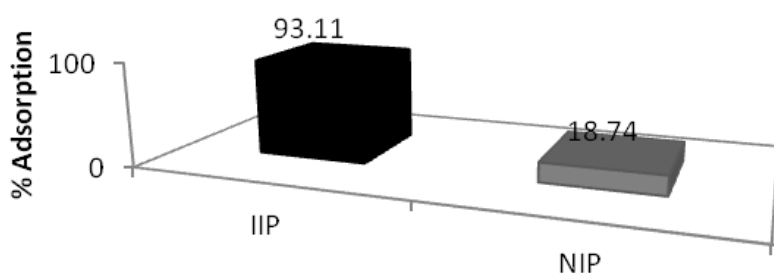


Figure 9. Selective adsorption of U(VI) from certified reference material (experimental conditions: $C_{U(VI)} = 0.93$ ppm (in the SRM), pH = 5.0, flow rate = 1 mL.min⁻¹, T = 25 °C)

Conclusions

We have shown that U(VI)-imprinted cryogel polymer (IIP) that contains Poly-Hydroxyethyl Methacrylate-Methacryloyl-L-Histidine is selective and has high adsorption capacity for U(VI) ion. A High adsorption rate was observed at the beginning of the adsorption process and saturation values are reached within 60 min. The maximum U(VI) adsorption capacity of the cryogel polymer was 74.80 mg.g⁻¹ for U(VI)-imprinted cryogel polymer, while that of non-imprinted cryogel polymer (NIP) was 14.76 mg.g⁻¹. The adsorption amount of U(VI) was maximum at pH 7.0. Competitive adsorption studies showed that, U(VI)-imprinted p-HEMA(MAH)₃ are only selective to U(VI) ion, even in the presence of other lanthanide ions such as, Nd(III), La(III) and Y(III) ions. Distribution (K_d), selectivity (k), and relative selectivity (k') coefficients were also calculated. The value of k' was found, 129, 60, and 79 for Nd(III), La(III), and Y(III), respectively. These k' values are high values if they are compared with reported research values. The obtained adsorption order under competitive conditions was U(VI) > La(III) > Y(III) > Nd(III). As a result, in our study to selectively remove the uranium used as fuel in nuclear reactors, it was determined that the prepared uranium-imprinted polymer exhibited effective uranium bonding activity and thus selectively separated from the matrix environment where uranium was found. After this stage, it is advisable to use sustainable membranes to purify the separated uranium and make it ready for use in the reactors (Fodi et al., 2017).

REFERENCES

- [1] Abdollahy M., Shojaosadati S. A., Tavakoli H. Z., Valivand A. (2011): Bioleaching of low grade uranium ore of Saghand Mine. – *Iranian Journal of Chemistry and Chemical Engineering* 10: 71-79.
- [2] Alvarez-Lorenzo C., Concheiro A. (2004): Molecularly imprinted polymers for drug delivery. – *Journal of Chromatography B* 804: 231-245.
- [3] Baysal Z., Aksoy E., Dolak I., Ersöz A., Say R. (2018): Adsorption behaviours of lysozyme onto poly-hydroxyethyl methacrylate cryogels containing methacryloyl antipyrine-Ce(III). – *International Journal of Polymeric Materials and Polymeric Biomaterials* 67: 199-204.
- [4] Bereli N., Saylan Y., Uzun L., Say R., Denizli A. (2011): L-Histidine imprinted supermacroporous cryogels for protein recognition. – *Separation and Purification Technology* 82: 28-35.
- [5] Candan N., Tüzmen N., Andaç M., Andaç C. A., Say R., Denizli A. (2009): Cadmium removal out of human plasma using ion-imprinted beads in a magnetic column. – *Materials Science and Engineering C* 29: 144-152.
- [6] Chen F., Yang Z., Tang Y., Wang X. (2017): Selective extraction and determination of di(2-ethylhexyl) phthalate in aqueous solution by HPLC coupled with molecularly imprinted solid-phase extraction. – *Iranian Journal of Chemistry and Chemical Engineering* 36: 127-136.
- [7] Chmielewski, A. G. (2008): Nuclear fissile fuels worldwide reserves. – *Nukleonika* 53: 11-14.
- [8] Dhal, P. K., Arnold, F. H. (1992): Metal-coordination interactions in the template-mediated synthesis of substrate-selective polymers: recognition of bis(imidazole) substrates by copper(II) iminodiacetate containing polymers. – *Macromolecules* 25: 7051-7059.
- [9] Didaskalou, C., Buyuktiryaki, S., Kecili, R., Fonte, C. P., Szekely, G. (2017): Valorisation of agricultural waste with an adsorption/nanofiltration hybrid process: from materials to sustainable process design. – *Green Chemistry* 19: 3116-3125.
- [10] Dolak, I. (2018): Selective separation and preconcentration of thorium (IV) in Bastnaesite ore using thorium (IV)-imprinted cryogel polymer. – *Hacettepe Journal of Biology and Chemistry* 46: 187-197.
- [11] Dolak, I., Tegin, I., Guzel, R., Ziyadanogulları, R. (2010): Removal and preconcentration of Pb(ii), Cr(iii), Cr(vi) from the aqueous solution and speciation of Cr(III)-Cr(VI)- by using functionalized amberlite XAD-16 resin with dithioethylenediamine. – *Asian Journal of Chemistry* 22: 6117-6124.
- [12] Dolak, I., Karakaplan, M., Ziyadanogulları, B., Ziyadanogulları, R. (2011): Solvent extraction, preconcentration and determination of thorium with monoaza 18-Crown-6 derivative. – *Bulletin of the Korean Chemical Society* 32: 1564-1568.
- [13] Dolak, I., Keçili, R., Hür, D., Ersöz, A., Say, R. (2015): Ion-imprinted polymers for selective recognition of neodymium (III) in environmental samples. – *Industrial & Engineering Chemistry Research* 54: 5328-5335.
- [14] Dolak, I., Keçili, R., Onat, R., Ziyadanoğulları, B., Ersöz, A., Say, R. (2018): Molecularly imprinted affinity cryogels for the selective recognition of myoglobin in blood serum. – *Journal of Molecular Structure* 1174: 171-176.
- [15] Fayazi, M., Ghanei, M. M., Taher, M. A., Ghanei-Motlagh, R., Salavati, M. R. (2016): Synthesis and application of a novel nanostructured ion-imprinted polymer for the preconcentration and determination of thallium(I) ions in water samples. – *Journal of Hazardous Materials* 309: 27-36.
- [16] Fodi, T., Didaskalou, C., Kupai, J., Balogh, G. T., Huszthy, P., Szekely, G. (2017): Nanofiltration-enabled in situ solvent and reagent recycle for sustainable continuous-flow synthesis. – *Chem Sus Chem* 10: 3435-3444.

- [17] Gao, B., Meng, J., Xu, Y., Zhang, Y. (2015): Preparation of Fe(III) ion surface-imprinted material for removing Fe(III) impurity from lanthanide ion solutions. – *Journal of Industrial Engineering and Chemistry* 24: 351-358.
- [18] Gu, Z. (2007): Probing the problems of thorium utilization as a nuclear energy resource. – *Chinese Journal of Nuclear Science and Engineering* 27: 97-105.
- [19] Haerizade, B. N., Ghavami, M., Koohi, M., Darzi, S. J., Rezaee, N., Kasaei, M. Z. (2018): Green removal of toxic Pb(II) from water by a novel and recyclable Ag/ γ -Fe₂O₃@r-GO nanocomposite. – *Iranian Journal of Chemistry and Chemical Engineering* 37: 29-37.
- [20] Harkins, D. A., Schweitzer, G. K. (1991): Preparation of site-selective ion-exchange resins. – *Separation Science and Technology* 26: 345-354.
- [21] Horwitz, E. P., Dietz, M. L., Chiarizia, R., Diamond, H., Essling, A. M., Graczyk, M. (1992): Separation and preconcentration of uranium from acidic media by extraction chromatography. – *Analytica Chimica Acta* 266: 25-37.
- [22] Iliia, R., Liatsou, I., Savva, I., Vasile, E., Vekas, L., Marinica, O., Mpekris, F., Pashalidis, I., Christoforou, T. K. (2017): Magneto-responsive polymer networks as adsorbents for the removal of U(VI) ions from aqueous media. – *European Polymer Journal* 97: 138-146.
- [23] İnam, R., Çaykara, T., Özyürek, C. (2001): Polarographic determination of uranyl ion adsorption on poly-(2-hydroxyethyl methacrylate/itaconic acid) hydrogels. – *Separation Science and Technology* 36: 1451-1461.
- [24] Kaminski, M. D., Nunez, L. (2000): Separation of uranium from nitric- and hydrochloric-acid solutions with extractant-coated magnetic microparticles. – *Separation Science and Technology* 35: 2003-2018.
- [25] Keçili, R., Dolak, I., Ziyadanoğulları, B., Ersöz, A., Say, R. (2018): Ion imprinted cryogel-based supermacroporous traps for selective separation of cerium (III) in real samples. – *Journal of Rare Earths* 36: 857-862.
- [26] Kupai, J., Razali, M., Buyuktiryaki, S., Kecili, R., Szekely, G. (2017): Long-term stability and reusability of molecularly imprinted polymers. – *Polymer Chemistry* 8: 666-673.
- [27] Lasáková, M., Jandera, P. (2009): Molecularly imprinted polymers and their application in solid phase extraction. – *Journal of Separation Science* 32: 788-812.
- [28] Li, F., Yang, Z., Weng, H., Chen, G., Lin, M., Zhao, C. (2018): High efficient separation of U(VI) and Th(IV) from rare earth elements in strong acidic solution by selective sorption on phenanthroline diamide functionalized graphene oxide. – *Chemical Engineering Journal* 332: 340-350.
- [29] Lu, Y., Wei, H., Zhang, Z., Li, Y., Wu, G., Liao, W. (2016): Selective extraction and separation of thorium from rare earths by a phosphorodiamidate extractant. – *Hydrometallurgy* 163: 192-197.
- [30] Mitreva, M., Dakova, I., Karadjova, I. (2017): Iron(II) ion imprinted polymer for Fe(II)/Fe(III) speciation in wine. – *Microchemica Journal* 132: 238-244.
- [31] Monier, M., Abdel-Latif, D. A. (2017): Fabrication of Au(III) ion-imprinted polymer based on thiol-modified chitosan. – *International Journal of Biological Macromolecules* 105: 777-787.
- [32] Monier, M., Abdel-Latif, D. A., Abou El-Reash, Y. G. (2016): Ion-imprinted modified chitosan resin for selective removal of Pd(II) ions. – *Journal of Colloidal and Interface Science* 469: 344-354.
- [33] Moorthy, M. S., Tapaswi, P. K., Park, S. S., Mathew, A., Cho, H.-J., Ha, C.-S. (2013): On-imprinted mesoporous silica hybrids for selective recognition of target metal ions. – *Microporous and Mesoporous Materials* 180: 162-171.
- [34] Moussa, M., Pichon, V., Mariet, C., Vercouter, T., Delaunay, N. (2016): Potential of ion imprinted polymers synthesized by trapping approach for selective solid phase extraction of lanthanides. – *Talanta* 161: 459-468.

- [35] Msaadi, R., Ammar, S., Chehimi, M. M., Yagci, Y. (2017): Diazonium-based ion-imprinted polymer/clay nanocomposite for the selective extraction of lead(II) ions in aqueous media. – *European Polymer Journal* 89: 367-380.
- [36] Pakdehi, S. G. (2016): Adsorptive removal of Al, Zn, Fe, Cr and Pb from hydrogen peroxide solution by IR-120 cation exchange resin. – *Iranian Journal of Chemistry and Chemical Engineering* 11: 75-84.
- [37] Panahi, H. A., Zadeh, M. S., Tavangari, S., Moniri, E., Ghassemi, J. (2012): Nickel adsorption from environmental samples by ion imprinted aniline -formaldehyde polymer. – *Iranian Journal of Chemistry and Chemical Engineering* 31: 35-44.
- [38] Roushani, M., Abbasi, S., Khani, H., Sahraei, R. (2015): Synthesis and application of ion-imprinted polymer nanoparticles for the extraction and preconcentration of zinc ions. – *Food Chemistry* 173: 266-273.
- [39] Sana, S., Roostaazad, R., Yaghmaei, S. (2015): Biosorption of uranium (VI) from aqueous solution by pretreated *aspergillus niger* using sodium hydroxide. – *Iranian Journal of Chemistry and Chemical Engineering* 8: 65-74.
- [40] Saylan, Y., Yilmaz, F., Özgür, E., Derazshamshir, A., Yavuz, H., Denizli, A. (2017): Molecular imprinting of macromolecules for sensor applications. – *Sensors* 17: 1-30.
- [41] Sellergren, B. (2001): Imprinted chiral stationary phases in high-performance liquid chromatography. – *Journal of Chromatography A* 906: 227-252.
- [42] Székely, G., Bandarra, J., Heggie, W., Sellergren, B., Ferreira, F. C. (2012b): A hybrid approach to reach stringent low genotoxic impurity contents in active pharmaceutical ingredients: Combining molecularly imprinted polymers and organic solvent nanofiltration for removal of 1,3-diisopropylurea. – *Separation and Purification Technology* 86: 79-87.
- [43] Székely, G., Fritz, E., Bandarra, J., Heggie, W., Sellergren, B. (2012a): Removal of potentially genotoxic acetamide and arylsulfonate impurities from crude drugs by molecular imprinting. – *Journal of Chromatography A* 1240: 52-58.
- [44] Vedadghavami, A., Minoei, F., Hosseini, S. S. (2018): Practical techniques for improving the performance of polymeric membranes and processes for protein separation and purification. – *Iranian Journal of Chemistry and Chemical Engineering* 37: 1-23.
- [45] Vidyasankar, S., Arnold, F. H. (1995): Molecular imprinting: Selective materials for separations, sensors and catalysis. – *Current Opinion in Biotechnology* 6: 218-224.
- [46] Wang, J., Chen, Z., Shao, D., Li, Y., Xu, Z., Cheng C, Asiri, A. M., Marwani, H. M., Hu, S. (2017a): Adsorption of U(VI) on bentonite in simulation environmental conditions. – *Journal of Molecular Liquids* 242: 678-684.
- [47] Wang, Y., Wu, L., Yang, Y., Feng, W., Yuan, L. (2015): Efficient separation of thorium from rare earths with a hydrogen-bonded oligoamide extractant in highly acidic media. – *Journal of Radioanalytical Nuclear Chemistry* 305: 543-549.
- [48] Wang, Y. L., Huang, C., Li, F. J., Dong, Y. M., Sun, X. Q. (2017b): Process for the separation of thorium and rare earth elements from radioactive waste residues using Cyanex® 572 as a new extractant. – *Hydrometallurgy* 169: 158-164.
- [49] Wei, S., Mizaiakoff, B. (2007): Recent advances on noncovalent molecular imprints for affinity separations. – *Journal of Separation Science*. 30: 1794-1805.
- [50] Wulff, G. (1995): Molecular imprinting in cross-linked materials with the aid of molecular templates—a way towards artificial antibodies. – *Angewandte Chemie International Edition* 34: 1812-1832.
- [51] Yener, I., Oral, E. V., Dolak, I., Ozdemir, O., Ziyadanogulları, R. (2017): A new method for preconcentration of Th (IV) and Ce (III) by thermophilic *Anoxybacillus flavithermus* immobilized on Amberlite XAD-16 resin as a novel biosorbent. – *Ecological Engineering* 103: 43-49.
- [52] Zhu, Z., Pranolo, Y., Cheng, C. Y. (2015): Separation of uranium and thorium from rare earths for rare earth production - a review. – *Mineral Engineering* 77: 185-196.